JOURNAL OF RAMAN SPECTROSCOPY
J. Raman Spectrosc. 2008; **39**: 61–67
Published online 26 November 2007 in Wiley InterScience
(www.interscience.wiley.com) DOI: 10.1002/jrs.1814

JRS

SERS intensity optimization by controlling the size and shape of faceted gold nanoparticles

Alia Sabur, Mickael Havel and Yury Gogotsi*

Materials Science and Engineering Department and the A.J. Drexel Nanotechnology Institute, Drexel University, 3141 Chestnut Street, Philadelphia, PA 19104, USA

Received 10 April 2007; Accepted 11 June 2007

In this work, we experimentally investigated the surface-enhanced Raman spectroscopy (SERS) activity of faceted gold nanoparticles, which have been theoretically predicted to yield giant enhancements. Glycine was used to determine the SERS activity as a function of pH and ionic strength and to estimate the corresponding enhancement factor (EF). By optimizing the synthesis conditions of the flat prismatic nanoparticles, it was possible to control their size and shape. We demonstrate that the maximum SERS intensity increases with the edge length of the triangle, reaching a maximum EF of $\sim 10^{13}$ for 1.9 μm triangles (the largest tested). The corresponding glycine detection limit was as low as 10^{-12} M, close to the single-molecule threshold. Copyright © 2007 John Wiley & Sons, Ltd.

KEYWORDS: SERS; gold; nanoparticles; glycine; enhancement factor

INTRODUCTION

Surface-enhanced Raman spectroscopy (SERS) is a technique that is generally used to enhance Raman signals by factors of 10^4–10^6.[1–3] The main purpose is to detect the weak Raman signal of molecules at low concentrations or having a low Raman scattering cross-section. In addition, SERS gives the possibility to acquire information specifically from the surface of materials (e.g. monolayers). Another advantage of SERS is that the spatial resolution is determined not by the diffraction limit, but by the spatial confinement of the local electric fields in the vicinity of nanoparticles.[4] This trace analytical capability at the nanoscale can be used, for example, to track the migration of molecules inside cells and to design integrated cellular probes.[5]

Two main mechanisms are responsible for SERS enhancement, electromagnetic and chemical.[6–9] The electromagnetic enhancement involves the excitation of surface plasmons on metal structures, while the chemical enhancement involves the formation of a charge-transfer complex between the metal and the analyte. It has been proposed that the chemical and electromagnetic mechanisms contribute to the total enhancement factor (EF) by 10^2 and 10^4, respectively. Single-molecule detection has been reported[10,11] with EFs as large as 10^{14}. To explain this enormous enhancement, other mechanisms, such as the quadrupole effect, must be considered.[12–14] On the basis of the quadrupole theory, it has been demonstrated that owing to the strong polarization at the tips of the particles, molecules are attracted to these areas where the electric field strength strongly increases, resulting in increased EF. It should be mentioned that strong electric fields can cause significantly altered selection rules[12,13] leading to the appearance of forbidden Raman lines, explaining some of the changes observed in the SER spectra compared to regular Raman spectra. The relaxation of the selection rules can also be explained by the gradient field effect.[12,15,16] While in regular Raman scattering the electric field is constant over the length of a chemical bond, in SERS it can vary because of the nanoscale gradient of the electric field associated with the localized surface plasmon.[17]

Generally, roughened metal plates or spherical nanoparticles are used for SERS. A strong disadvantage of using nanospheres is that the particles need to be in groups and form the so-called 'hot spots' to obtain significant EFs. This requires a fine control over the aggregation of the particles, leading to nonuniform, localized and often time-limited[2] excitation. When the nanoparticles aggregate, the individual dipole oscillators of the particles couple, generating normal modes of plasmon excitation that embrace the cluster and cover a very broad range of frequencies.[4] In addition, only 1 in every 100–1000 nanoparticles is 'optically hot' and only 1 in every 10 000 surface sites on a 'hot' particle produces efficient enhancement.[18] Faceted nanoparticles can create these hot spots individually, removing the need for precise control of aggregation.[19]

*Correspondence to: Yury Gogotsi, Materials Science and Engineering Department and the A.J. Drexel Nanotechnology Institute, Drexel University, 3141 Chestnut Street, Philadelphia, PA 19104, USA. E-mail: gogotsi@drexel.edu

JRS

Despite the advantages of faceted particles, which have been discussed theoretically in detail,[12,13,19–24] there have been very few papers experimentally validating the theory,[25,26] and the effects of particle size and shape have not been investigated. The aim of this study is to produce faceted gold particles and study the effect of their morphology on EF and SERS mechanism. Glycine was used as the SERS test molecule, as it is the simplest amino acid that has been characterized in detail with SERS previously.[2,27,28]

EXPERIMENTAL

Glycine ($C_2H_5NO_2$) was purchased from Sigma Co. and used without further purification. The typical concentration used was 1 mM, with different concentrations used to determine the EF. Since it has been demonstrated that a strong SERS effect could be observed for a longer period of time when the pH of the solution is adjusted around the isoelectric point of glycine (6.06),[2] the pH was adjusted to 6 by addition of HCl. The effects of both pH and NaCl concentration on SERS intensity are studied in this work.

Raman spectra were acquired using a Renishaw 1000/2000 Raman micro-spectrometer (1200 l/mm grating) in backscattering geometry. The excitation source was a diode laser (785 nm), focused with a 50× long-local-length objective to a spot size of approximately 2 m and providing a power of 2 mW on the sample. The spectra were analyzed using the Wire 2.0 software from Renishaw. For all Raman and SER spectra, the intensities are plotted in counts per second (cps). A Zeiss Supra 50VP instrument was used to obtain scanning electron microscopy (SEM) images. UV-vis spectra were recorded using a Perkin Elmer, UV/Vis Lambda 35 spectrometer.

RESULTS AND DISCUSSION

Preparation of gold nanotriangles

Nanotriangles were synthesized on the basis of the method used by Rai *et al*.[29] Five grams of dried lemongrass leaves were finely cut, washed, and boiled in 20 ml of DI water for 5 min to obtain the leaf extract. Ten milliliters of a 1 mM aqueous $HAuCl_4$ solution was mixed with different amounts of the lemongrass extract at room temperature, and stirred overnight. The solutions were then allowed to rest at room temperature for 1 week to reach equilibrium. The gold solutions were then centrifuged at 8000 rpm for 5 min and redispersed in DI water. This procedure was repeated five times and the resulting solutions were used to obtain SER spectra.

The lemongrass extract contains sodium citrate, which reduces gold. It has been suggested that the slow reduction and the shape-directing ability of the carbonyl compounds present in the extract are responsible for the creation of triangles in the solution.[30,31] Samples from different extract concentration have been observed with SEM (Fig. 1). Apart from triangles, the synthesis process also yielded a large number of truncated triangles, hexagons, and small polyhedral particles. Gold particles have a broad size distribution, from ~20 nm to ~5 m, depending on the extract concentration, and are flat with heights up to 40 nm (Fig. 1(b)) except for small polyhedral, equiaxial particles. The triangles, truncated triangles, and hexagons are so thin that they are transparent to the electron beam at 10 kV (Fig. 1(a)).

SERS with gold nanotriangles

Gold particles were then used to record the SERS of a 1 mM glycine solution. At this concentration, glycine is not detectable by regular Raman spectroscopy (Fig. 2(a)) in solution. At a higher concentration (100 mM), Raman spectra of good quality can be recorded in the macro mode, but a higher concentration was required to record a micro-Raman spectrum from a droplet on a Si wafer. For all SER spectra, a droplet of gold colloidal solution was allowed to dry on a silicon wafer. Subsequently, a drop of glycine solution was added on top of the substrate. The regular Raman and SERS peaks for glycine are assigned in Table 1. The differences between the regular Raman and SER spectra can be explained by the gradient field and quadrupole effects, as discussed above. In Fig. 2(b), the most intense peak is located at 734 cm^{-1}, which we assign to the bending

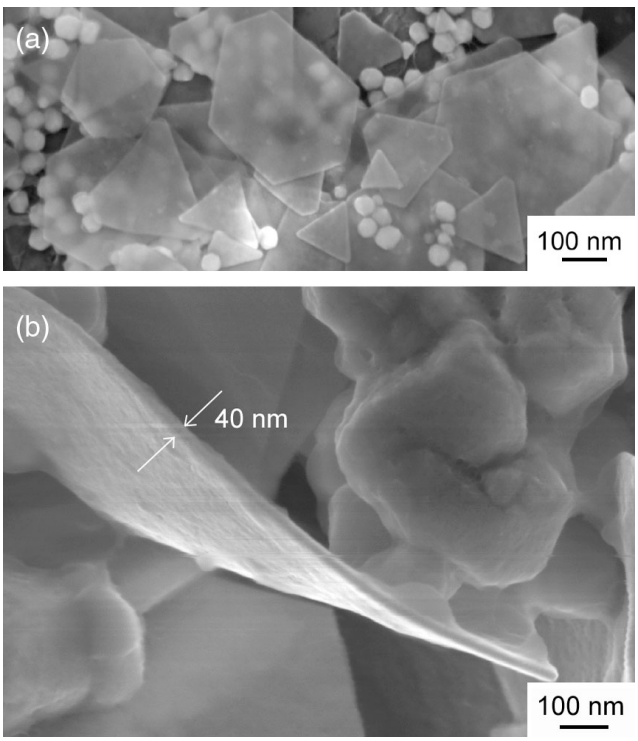

Figure 1. SEM images of (a) a typical sample (4.8 vol% extract) containing triangular, hexagonal, and uniaxial nanoparticles. (b) a large gold platelet showing the thickness (~40 nm), from the 0.74 vol% extract sample.

DOI: 10.1002/jrs

vibration of NH_2 groups. Indeed, Dou *et al*.[2] demonstrated that glycine interacts with gold nanoparticles through the amino groups, which are therefore more affected by the plasmon-generated electric field. Furthermore, Kumar *et al*.[32] calculated the position of this vibration by the *ab initio* method and found a position at 720 cm^{-1}, which was experimentally observed at 697 cm^{-1}. The other main peaks are located at 877 cm^{-1} (NH_2 twist), 962–1031 cm^{-1} (C–C and C–N stretch), 1317–1347 cm^{-1} (NH_2–CH_2 twist).

To evaluate the optimal extract concentration in terms of SERS intensity, spectra were recorded for the Au samples produced with 0.1 to ~30 vol% of lemongrass extract. Figure 3 shows some Raman spectra recorded using these gold samples showing the reproducibility of the spectra and also some variations in peak intensity and the number of peaks observed. The SERS intensities of the peak at 734 cm^{-1} with respect to the concentration of lemongrass extract are reported in Fig. 4(a). The use of samples synthesized in two different experimental series (Fig. 4(a)) separated by two months shows the reproducibility of the process, which is often an issue when a natural precursor, such as lemongrass, is used. There is a clear maximum at 1 vol%, which coincides with the maximum edge length of the triangles (1.9 m, Fig. 4(b) and the corresponding SEM images in Fig. 5). It is also between 0.5 and 5 vol% that the highest concentration of triangles with respect to other shapes, i.e. truncated triangles and hexagons, was observed. It can be concluded that increasing the concentration and size of triangles leads to the optimal SERS conditions. This contrasts with other studies in which a maximum of SERS intensity was identified for ~80–100 nm Ag nanoparticles.[11,18]

Table 1. Raman peaks and the corresponding assignments in the conventional and SER spectra of Glycine according to Refs 2, 27 and 28 (for the intensities, s = strong, m = medium, w = weak)

Regular Raman	SERS	Assignment
	618 w	COOH bend
	734 s	NH_2 bend
	877 m	NH_2twist + CH_2 twist
901 s	962 m	C–C stretch
1033 w	1016 w, 1031 w	C–N stretch
1131 w	1169 m, 1117 w	NH_3^+ wag
	1236 m	
1328 s	1317 m	CH_2 wag
	1347 m	C–NH_3^+ stretch
1407 s	1406 w	COOH sym. stretch
1438 m	1462 w	CH_2 bend
1513 w	1543 w	NH_3^+ sym. def.
	1573 w, 1599 w	COOH asym. stretch
1612 m		NH_3^+ asym. def.

The charge of both gold nanoparticles and glycine molecules is a key factor for the optimization of the SERS intensity. Because it depends on both pH (Eqn (1)) and ionic strength, we investigated the SERS intensity as a function of these two parameters (Fig. 6).

$$^{+}NH_3{-}CH_2{-}COOH \xrightleftharpoons{pK_1=2.3} NH_2{-}CH_2{-}COOH \xrightleftharpoons{pK_2=9.8} NH_2{-}CH_2{-}COO^{-} \quad (1)$$

As expected, the SERS intensity increases significantly with decreasing pH, indicating that the protonated amino groups interact preferentially with the negatively charged gold particles. This result is in good agreement with previous work.[1,2,27] Furthermore, the SERS intensity increases with the ionic strength (NaCl concentration from 1 to 58 mM), suggesting an increased attraction between the glycine molecules and the nanoparticles. Thus, further increase in SERS signal intensity can be achieved between the glycine molecules and the nanoparticles.

It is known that the optical properties of nanoparticles are an important factor in the SERS activity. It has been demonstrated that the nanoparticle size and shape strongly influence the plasmon excitation.[31] For this reason, the optical properties of the gold nanoparticles were investigated.

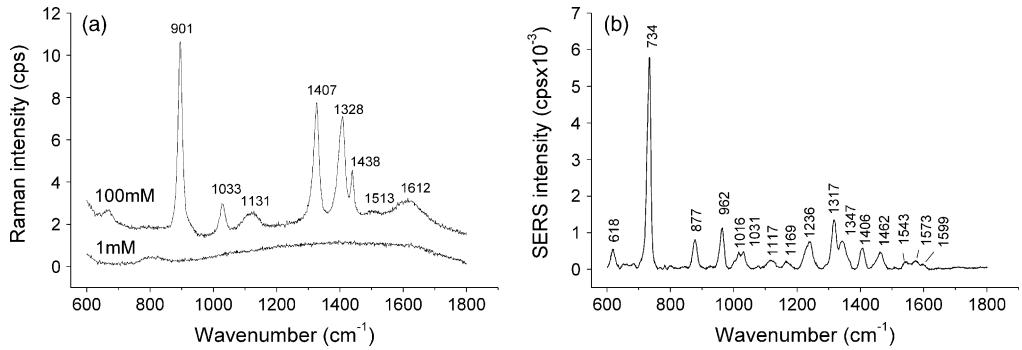

Figure 2. (a) Regular Raman spectra of 1 and 100 mM of glycine (1500 s); (b) SER spectrum of 1 mM glycine using the 1 vol% extract nanotriangle sample (10 s).

DOI: 10.1002/jrs

JRS

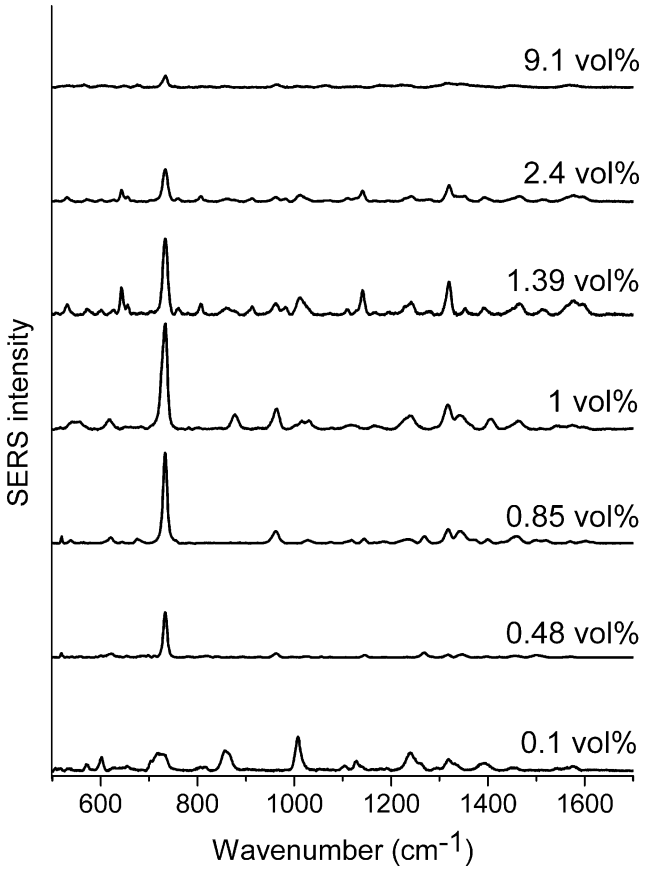

Figure 3. Typical Raman spectra for 1 mM glycine with triangles prepared with a range of lemongrass extract concentrations. Acquisition time 10 s.

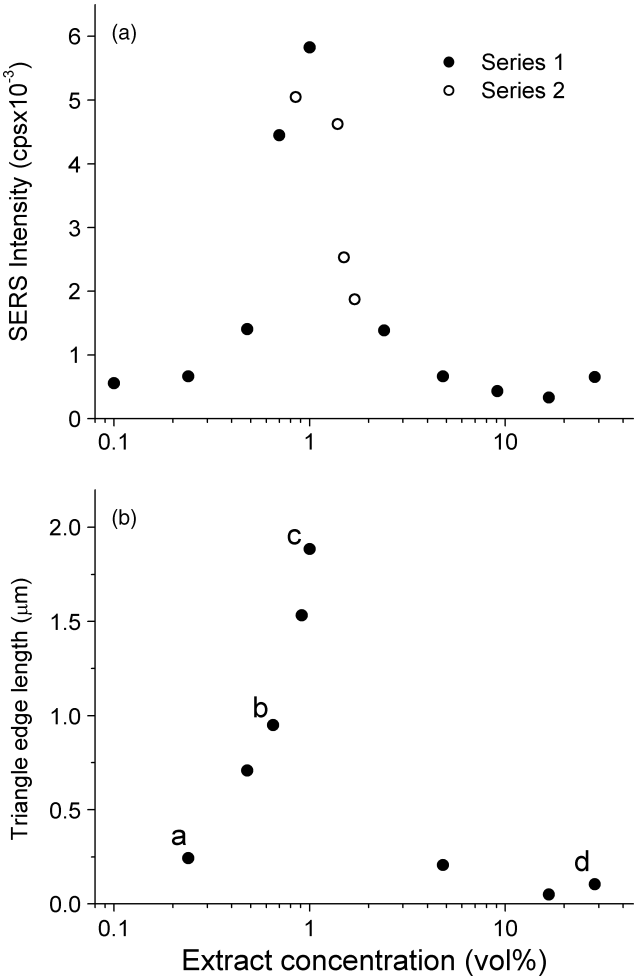

Figure 4. Dependence of (a) SERS intensity of the 734 cm^{-1} peak (two series of samples were synthesized independently under the same conditions, showing the reproducibility of the method) and (b) triangle edge length on the concentration of lemongrass extract. The labels a–d correspond to the SEM images shown in Fig. 5.

Figure 7 shows UV-vis absorption spectra of three different samples. For the 1 vol% sample, which corresponds to the maximum SERS intensity, the plasmon peak is very broad, from ~550 to ~1100 nm. This has been shown to correspond with the coupling of plasmon modes in clusters of nanoparticles.[4]

To determine the EF and detection limit provided by the faceted particles of the optimal shape, SER spectra were recorded for different concentrations of glycine (Fig. 8). The sample data followed a log–log linear model for concentrations between 10^{-10} and 10^{-3} M, indicating that quantitative analysis would be possible in that range. The determination of the detection limit was done by extrapolation from Fig. 8. Assuming that a detection limit of ~1 cps is desired for any analyte, we find that the minimum concentration of glycine to reach this limit is 10^{-12} M, which is close to the single-molecule detection limit. Indeed, Eggeling *et al.*[33] and Kneipp *et al.*[10] claimed that they achieved single-molecule SERS detection with analyte concentrations as low as 10^{-12} and 3×10^{-14} M, respectively.

To determine the peak EF, the equation proposed by McFarland *et al.*[34] has been used:

$$EF = I_{SERS}N_{RR}/(I_{RR}N_{SERS}) \quad (2)$$

where N_{RR} and N_{SERS} are the number of molecules probed by regular Raman spectroscopy and SERS, respectively, and I_{RR} and I_{SERS} are the corresponding intensities. To calculate the EF, it is critical to estimate the volumes probed by the two methods. In the case of regular Raman spectroscopy, we assume that the volume probed is a cylinder of 2×5 m (provided by a 50× objective in the confocal mode with an aperture of 50 m), giving a volume of 15.7 fl. Therefore, a glycine concentration of 0.5 M corresponds to $\sim 5 \times 10^9$ molecules in this volume, giving a Raman intensity of 4 cps. In the case of SERS, we assume that the signal comes only from the triangle-rich areas and that those areas represent 10% of coverage. The analyzed volume on the gold-coated silicon wafer can be considered as a cylinder of 2×0.1 m (we assume that the electric field coming from the triangles does not extend to a distance higher than 100 nm), giving a

DOI: 10.1002/jrs

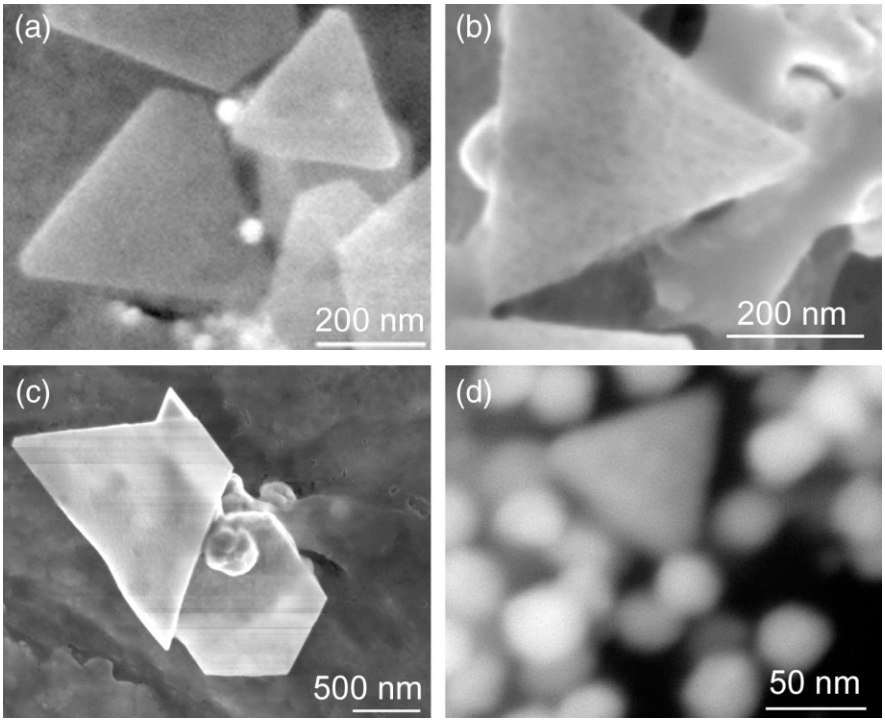

Figure 5. SEM images of gold nanotriangles synthesized from 0.1, 0.5, 1.0, and 28.6 vol% of lemongrass extract, from (a) to (d), respectively. The labels correspond to the letters indicated in Fig. 4(b).

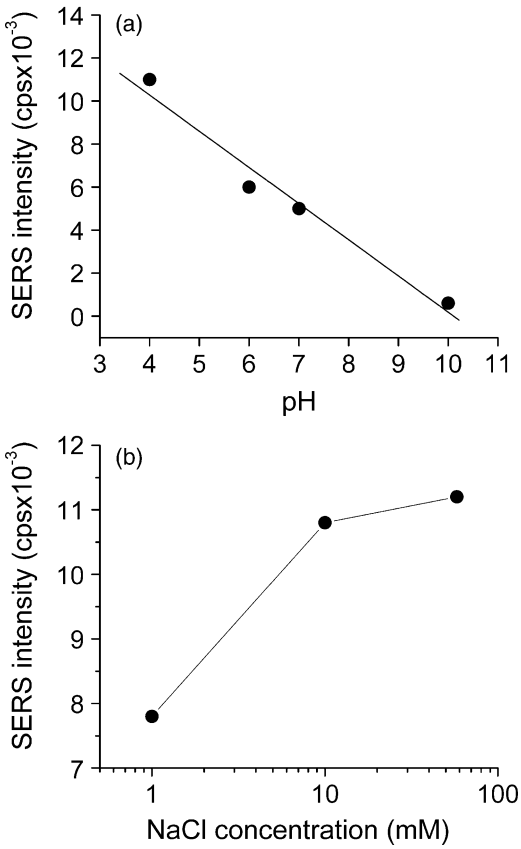

Figure 6. Dependence of the SERS intensity of the 734 cm^{-1} peak on (a) pH in a 10 mM NaCl solution and (b) NaCl concentration at pH 4 (1 mM solution, acquisition time 10 s).

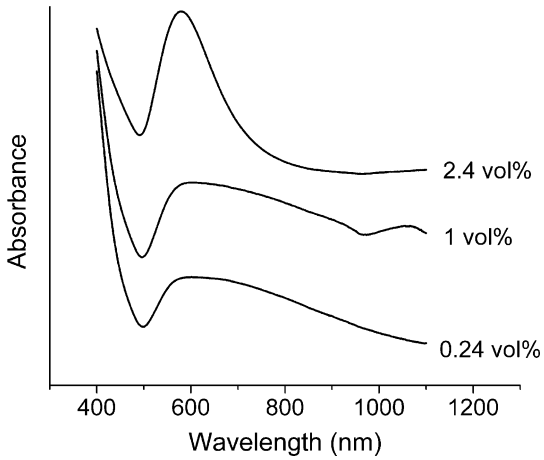

Figure 7. UV-vis absorption spectra of nanotriangle samples produced using lemongrass extract of three different concentrations.

volume of 3×10^{-2} fl. Then, at a 10^{-10} glycine concentration, $\sim 2 \times 10^{-3}$ molecules are probed in this volume, producing a SERS intensity of 5 cps. Note that this value, which is lower than one molecule in the analyzed volume, is still sufficient to provide a recordable SERS signal. This can be explained by molecular migration due to Brownian motion and/or adsorption of glycine molecules on gold. Indeed, in a typical SERS experiment, a droplet of about 20 l was deposited on the Si substrate. This droplet contains, at 10^{-10} M glycine concentration, around 10^9 molecules. From these parameters,

DOI: 10.1002/jrs

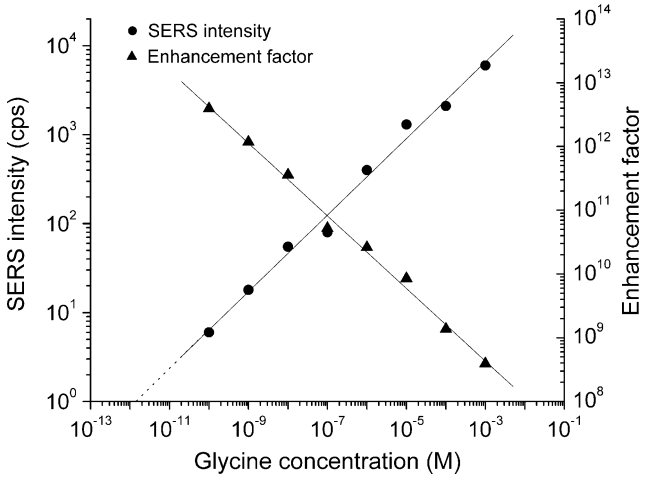

Figure 8. Logarithmic plot of the SERS intensity (734 cm^{-1} peak) and enhancement factor with respect to the glycine concentration.

we obtain an EF = $(5 \times 5 \times 10^9)/(4 \times 2 \times 10^{-3}) \approx 3 \times 10^{12}$.

The EF corresponding to the different glycine concentrations has been calculated and reported in Fig. 8. The range of EFs possible spans a few orders of magnitude. It is interesting to note that it is strongly dependent on the glycine concentration, going from 10^8 (10^{-3} M) to 10^{12} (10^{-10} M). Even at the lowest point, there are still several orders of magnitude of enhancement.

Thus, using a concentration other than the minimum detectable will give a lower value for the EF – this is why 'peak' EFs are typically calculated.[34] These measure the highest EF achievable with the particular method in use.

To explain the variation of the EF with the glycine concentration, we need to consider quadrupole interactions. According to Polubotko,[13] molecules in the vicinity of particles' tips and wedges show an increased polarization. The molecules are then attracted to these locations of minimal potential energy, causing enormous enhancements. In this scenario, as the molecules get closer to the particles, the EF increases because of the stronger electric field. In the case of low concentration SERS experiments, it is likely that monolayers of glycine adsorb on the particles and benefit from the strongest electric field. However, as the concentration increases, secondary layers of glycine molecules with salvation shells surround the particles. Each successive layer will experience a weakening electric field as the distance to the particle increases. This phenomenon may explain why as the glycine concentration increases, the total SERS intensity increases but the EF decreases, as shown in Fig. 8.

CONCLUSIONS

This study confirms theoretical predictions that faceted nanoparticles would yield very large enhancements, with an increase in signal up to 10^{13}. It is also demonstrated that SERS intensity strongly increases with the size of the nanotriangles. The largest triangles tested (1.9 m) gave a SERS intensity of 6×10^3 cps. We report that the minimal concentration of glycine to be measured by this technique is 10^{-12} M, close to the single-molecule detection threshold. A dependence of the EF on the analyte concentration has been demonstrated.

Acknowledgements

The authors would like to thank Dee Breger and Davide Mattia for operating the SEM, and Guzeliya Korneva for assistance in performing UV-vis spectroscopy. Alia Sabur was supported by an NDSEG Fellowship and a Dean's Fellowship. Mickael Havel was supported by an Arkema postdoctoral fellowship. Raman spectroscopy and SEM studies were performed at the Centralized Materials Characterization Facility of the A.J. Drexel Nanotechnology Institute.

REFERENCES

1. Hildebrandt P, Stockburger M. *J. Phys. Chem. B* 1984; **88**: 5935.
2. Dou XM, Jung YM, Cao ZQ, Ozaki Y. *Appl. Spectrosc.* 1999; **53**: 1440.
3. Xu HX, Aizpurua J, Kall M, Apell P. *Phys. Rev. E* 2000; **62**: 4318.
4. Kneipp K, Kneipp H, Itzkan I, Dasari RR, Feld MS. *J. Phys.: Condens. Matter* 2002; **14**: R597.
5. Mattia D, Korneva G, Sabur A, Friedman G, Gogotsi Y. *Nanotechnology* 2007; **18**: 155 305.
6. Moskovits M. *Rev. Mod. Phys.* 1985; **57**: 783.
7. Otto A, Mrozek I, Grabhorn H, Akemann W. *J. Phys.: Condens. Matter* 1992; **4**: 1143.
8. Campion A, Ivanecky JE, Child CM, Foster M. *J. Am. Chem. Soc.* 1995; **117**: 11 807.
9. Campion A, Kambhampati P. *Chem. Soc. Rev.* 1998; **27**: 241.
10. Kneipp K, Wang Y, Kneipp H, Perelman LT, Itzkan I, Dasari R, Feld MS. *Phys. Rev. Lett.* 1997; **78**: 1667.
11. Emory SR, Nie S. *J. Phys. Chem. B* 1998; **102**: 493.
12. Polubotko AM. *Phys. Lett. A* 1990; **146**: 81.
13. Polubotko AM. *J. Opt. A: Pure Appl. Opt.* 1999; **1**: L18.
14. Ayars EJ, Hallen HD, Jahncke CL. *Phys. Rev. Lett.* 2000; **85**: 4180.
15. Sass JK, Neff H, Moskovits M, Holloway S. *J. Phys. Chem. B* 1981; **85**: 621.
16. Moskovits M, Dilella DP. *J. Chem. Phys.* 1982; **77**: 1655.
17. Feibelman PJ. *Phys. Rev. B* 1975; **12**: 1319.
18. Nie S, Emory SR. *Science* 1997; **275**: 1102.
19. Haynes CL, McFarland AD, Van Duyne RP. *Anal. Chem.* 2005; **77**: 338A.
20. Yang WH, Schatz GC, Vanduyne RP. *J. Chem. Phys.* 1995; **103**: 869.
21. Kottman JP, Martin OJF, Smith DR, Schultz S. *Opt. Express* 2000; **6**: 213.
22. Haes AJ, Zou SL, Schatz GC, Van Duyne RP. *J. Phys. Chem. B* 2004; **108**: 6961.
23. Hao E, Schatz GC. *J. Chem. Phys.* 2004; **120**: 357.
24. Okada N, Hamanaka Y, Nakamura A, Pastoriza-Santos I, Liz-Marzan LM. *J. Phys. Chem. B* 2004; **108**: 8751.
25. Krug JT, Wang GD, Emory SR, Nie SM. *J. Am. Chem. Soc.* 1999; **121**: 9208.
26. dos Santos DS, Alvarez-Puebla RA, Oliveira ON, Aroca RF. *J. Mater. Chem.* 2005; **15**: 3045.
27. Dou XM, Jung YM, Yamamoto H, Doi S, Ozaki Y. *Appl. Spectrosc.* 1999; **53**: 133.

DOI: 10.1002/jrs

28. Podstawka E, Ozaki Y, Proniewicz LM. *Appl. Spectrosc.* 2005; **59**: 1516.
29. Rai A, Singh A, Ahmad A, Sastry M. *Langmuir* 2006; **22**: 736.
30. Shankar SS, Rai A, Ankamwar B, Singh A, Ahmad A, Sastry M. *Nat. Mater.* 2004; **3**: 482.
31. Shankar SS, Rai A, Ahmad A, Sastry M. *Chem. Mater.* 2005; **17**: 566.
32. Kumar S, Rai AK, Singh VB, Rai SB. *Spectrochim. Acta A Mol. Biomol. Spectrosc.* 2005; **61**: 2741.
33. Eggeling C, Schaffer J, Seidel CAM, Korte J, Brehm G, Schneider S, Schrof W. *J. Phys. Chem. A* 2001; **105**: 3673.
34. McFarland AD, Young MA, Dieringer JA, Van Duyne RP. *J. Phys. Chem. B* 2005; **109**: 11 279.

DOI: 10.1002/jrs